



**HAL**  
open science

## Propagation Failure by TRPM4 Overexpression

Namit Gaur, Thomas Hof, Michel Haïssaguerre, Edward Vigmond

► **To cite this version:**

Namit Gaur, Thomas Hof, Michel Haïssaguerre, Edward Vigmond. Propagation Failure by TRPM4 Overexpression. *Biophysical Journal*, 2019, 116 (3), pp.469-476. 10.1016/j.bpj.2018.11.3137. hal-02885623

**HAL Id: hal-02885623**

**<https://hal.science/hal-02885623>**

Submitted on 21 Oct 2021

**HAL** is a multi-disciplinary open access archive for the deposit and dissemination of scientific research documents, whether they are published or not. The documents may come from teaching and research institutions in France or abroad, or from public or private research centers.

L'archive ouverte pluridisciplinaire **HAL**, est destinée au dépôt et à la diffusion de documents scientifiques de niveau recherche, publiés ou non, émanant des établissements d'enseignement et de recherche français ou étrangers, des laboratoires publics ou privés.



Distributed under a Creative Commons Attribution - NonCommercial 4.0 International License

# Propagation Failure by TRPM4 Overexpression

N. Gaur<sup>1,2</sup>, T. Hof<sup>2</sup>, M. Haissaguerre<sup>2</sup>, and E.J. Vigmond<sup>1,2,\*</sup><sup>1</sup>Univ. Bordeaux, IMB UMR 5251, F-33400 Talence, France<sup>2</sup>IHU Liryc, Electrophysiology and Heart Modeling Institute, fondation Bordeaux Université, F-33600 Pessac- Bordeaux, France

\*Correspondence: edward.vigmond@u-bordeaux.fr

**ABSTRACT** Transient receptor potential melastatin member 4 (TRPM4) channels are non-selective monovalent cationic channels found in human atria and conduction system. Overexpression of TRPM4 channels has been found in families suffering from inherited cardiac arrhythmias, notably heart block. In this study, we integrate a mathematical formulation of the TRPM4 channel into a Purkinje cell model (Pan-Rudy(PRd) model). Instead of simply adding the channel to the model, a combination of existing currents equivalent to the TRPM4 current was constructed, based on TRPM4 current dynamics. The equivalent current was then replaced by the TRPM4 current in order to preserve the model action potential (AP). Single cell behavior showed early afterdepolarizations (EADs) for increases in TRPM4 channel expression above 2-fold. In a homogeneous strand of tissue, propagation conducted faithfully for lower expression levels, but failed completely for more than a doubling of TRPM4 channel expression. Only with a heterogeneous distribution of channel expression was intermittent heart block seen. This study suggests that in Purkinje fibres (PF), TRPM4 channels may account for sodium background current ( $I_{NaB}$ ), and that a heterogeneous expression of TRPM4 channels in the His/Purkinje system is required for type II heart block, as seen clinically.

## INTRODUCTION

The transient receptor potential melastatin 4 (TRPM4) channel is a homotetrameric nonselective channel permeable to monovalent cations but not to  $Ca^{2+}$  (permeability sequence:  $Na^+ \approx K^+ > Cs^+ > Li^+ \gg Ca^{2+}$ ) (1, 2). It harbors a linear unitary current-voltage relationship, a conductance of 20-25 pS (1), and its open probability increases with depolarization and intracellular  $Ca$  ( $Ca_i$ ) (3). At the whole-cell level, 10  $\mu M$   $Ca_i$  is sufficient to elicit a typical TRPM4 outward rectifying current in heterologous expression system, suggesting that physiological ranges of  $Ca_i$  rises (subsarcolemmal  $Ca_i$  of 10-15  $\mu M$  in cardiac cells (4)) are able to activate the channel. TRPM4 mRNA and protein is highly expressed in heart, especially in the conductive tissue. It participates in electrical activity of several cardiac structures including Purkinje fibers (PF) (5).

TRPM4 gene mutation was first reported as the cause of autosomal dominant form of progressive familial heart block type I (PFHBI) in a large Afrikaaner pedigree (6). Liu et al. (7) demonstrated three other TRPM4 mutations in familial cases of idiopathic cardiac conduction disease. Several other mutations have been found in families with autosomal dominant inherited conduction blocks, including bundle branch blocks (8–11). Most mutations result in impaired SUMOylation and endocytosis of TRPM4 channels resulting in overexpression of channel density and currents on the sarcolemma (6, 7, 11). Despite its role in regulating the conduction activity in PF and in causing inherited conduction blocks, the arrhythmogenic mechanisms behind such activity by TRPM4 channels remain elusive.

In this work, we develop a novel mathematical formulation of TRPM4 channel current using available experimental data on activation of TRPM4 channels by voltage and  $Ca_i$ . The channel current is integrated into a Purkinje cell ionic model (Pan-Rudy model (PRd)) (12). We investigate single cell behavior and propagation in a PF with a heterogeneous channel distribution. Results indicate that overexpression of TRPM4 channels can lead to early afterdepolarizations (EADs) in single cells. Only with a heterogeneous distribution of TRPM4 channels in PF, complex patterns of conduction blocks such as Type I, II, III, pacemaking activity and repolarization failure are observed. This study demonstrates mechanisms behind complex patterns of conduction block due to overexpression of TRPM4 channels. It also shows that background ionic currents in cell models may represent as yet uncharacterized currents.

## METHODS

### Channel formulation

TRPM4 gene encodes a non-selective cation channel that is roughly equally permeable to  $Na^+$  and  $K^+$  (13). TRPM4 current is sensitive to  $Ca_i$ , which activates the channel, and to voltage, which evokes higher activity in the positive voltage range (1, 14).

Inside-out patch clamp experiments of single channel activity revealed that the reversal potential of TRPM4 channel is close to zero (0.2 mV), indicating that the channel does not differentiate among monovalent cations (13). Mean open channel probability ( $P_o$ ) is an increasing function of membrane voltage, and the channel activity is higher at depolarized potentials. This data is fit to a Boltzmann function to develop a voltage activation gate of the channel. The  $EC_{50}$  of  $Ca_i$  activation is 1.3  $\mu$ M, close to peak systolic  $Ca_i$  values (15). Accordingly, we used this data to fit the calcium-activation gate for the channel. The channel opening is assumed to respond instantaneously to voltage and with a slower dynamics to  $Ca_i$  changes. Assembled together, the formulation for TRPM4 channel current can be written as:

$$I_{TRPM4} = \bar{g}_{TRPM4} \cdot X_{Cai} \cdot X_v \cdot (V - E_{TRPM4}) \quad (1)$$

$$= I_{Na,TRPM4} + I_{K,TRPM4} \quad (2)$$

$$\frac{dX_{Cai}}{dt} = \frac{X_{Cai}^{\infty} - X_{Cai}}{\tau_{X_{Cai}}} \quad (3)$$

$$X_v = 0.05 + \frac{0.95}{1 + e^{-(V-40)/15}} \quad (4)$$

$$X_{Cai}^{\infty} = \frac{1}{1 + ([Ca^{2+}]_{SSL}/0.0013)^{-1.1}} \quad (5)$$

$$\tau_{X_{Cai}} = 30 \quad (6)$$

$$I_{Na,TRPM4} = g_{Na,TRPM4} \cdot (V - E_{Na}) \quad (7)$$

$$I_{K,TRPM4} = g_{K,TRPM4} \cdot (V - E_K) \quad (8)$$

$V$  is the transmembrane voltage (mV),  $E_X$  is the reversal potential for species  $X$ .  $\bar{g}$  is the maximum conductance of the channel ( $mS/cm^2$ ), and  $\tau_{X_{Cai}}$  is the time constant for Ca-dependent changes (ms).  $X_v$  is the voltage activation gate and  $X_{Cai}$  the calcium activation gate. To decompose  $I_{TRPM4}$  into its constituent currents  $I_{Na,TRPM4}$  and  $I_{K,TRPM4}$ , we used the fact that at  $V = E_{TRPM4}$ ,  $I_{TRPM4} = 0$  to solve the conductance values for  $Na^+$  and  $K^+$  currents through TRPM4 channels:

$$g_{K,TRPM4} = I_{TRPM4} \cdot \frac{E_{TRPM4} - E_{Na}}{(V - E_{Na})(E_K - E_{TRPM4}) + (V - E_K)(E_{TRPM4} - E_{Na})} \quad (9)$$

$$g_{Na,TRPM4} = I_{TRPM4} \cdot \frac{E_K - E_{TRPM4}}{(V - E_{Na})(E_K - E_{TRPM4}) + (V - E_K)(E_{TRPM4} - E_{Na})} \quad (10)$$

The Pan-Rudy ionic model (PRd) of the canine Purkinje cell (12) was chosen for the study since it is the only model which captures the 3-tier  $Ca$ -release process, and TRPM4 channel opening is primarily dependent on  $Ca_i$ . The model prediction matches experimental data as shown in Fig. 1A. The species ionic currents ( $I_{Na,TRPM4}$ ,  $I_{K,TRPM4}$ ) are used to determine the balance of  $Na^+$  and  $K^+$  flowing through TRPM4 channels.  $Na^+$  flows into the subsarcolemma (SSL) and  $K^+$  into the bulk myoplasm of the Purkinje cell in PRd. Both cell and cable simulations were run till dynamic steady-state was reached and changes in state variables from beat to beat were  $<0.01\%$ .

## Cable behavior classification

The following are the definitions of cable behavior in Table 1. 1:1 refers to normal conduction along the cable. 1st degree block occurs when the impulse reaches the right end after a delay of more than 40 ms. Cable is quiescent when it cannot be excited. 2nd degree block occurs when some of the impulses fail to propagate to the right end. When no impulse reaches the right end, the cable has a 3rd degree block. If there are spontaneous APs in the cable, then the cable has a pacemaker behavior. If some APs in the left or right end nodes fail to repolarize before the impulse reaches the node, then the cable has repolarization failure. The criteria is applied sequentially from top to bottom of the table, so that there can only be one type of cable behavior. Thus, *eg.* cable cannot have both repolarization failure and a 2nd degree block.

## Software

The Cardiac Arrhythmia Research Package (CARP) was used for single cell and cable simulations (16). The bench module was used for single cell simulations. MagicPlot Student v2.7.2 and Grace v5.1.25 were used as plotting software. MATLAB R2015b was used for data analysis.

Figure 1: Validation of the TRPM4 channel current formulation in the Purkinje cell model (PRd). A. Model fit to experimental data on voltage-dependent activation (13) and Ca-dependent activation of the channel (15). The currents are normalized to correspond to normalized open probability  $P_o$  data. B. Rate dependence of original PRd (12) and PRd with TRPM4 channel current formulation for action potential duration (APD), max  $[Na^+]$  in the subsarcolemma ( $[Na^+]_{SSL}$ ), max  $[K^+]$  in the bulk myoplasm ( $[K^+]_i$ ), and max averaged  $[Ca^{2+}]$  ( $[Ca^{2+}]_{avg}$ ) agree with the original model values. Small differences occur at slow rates.  $[Ca^{2+}]_{avg}$  is the spatially averaged  $[Ca^{2+}]$  in peripheral coupling space (PCS), subsarcolemma (SSL) and bulk myoplasm (12)

## RESULTS

### Incorporation into an Existing Purkinje Cell Model

Published cell models are tuned to recreate measured experimental behavior. Of particular note is that TRPM4 channel block leads to a dramatic APD shortening (13). Hu *et al.* (17) have been the only group to add a TRPM4 channel current to several ionic models, but no attempt was made to adjust for control APs. Simply adding a current of such magnitude to existing models greatly affects the APs, such that AP no longer corresponds to the measured AP fitting data. See Fig. 2. Thus, it was reasoned that the effect of TRPM4 current had to have been implicitly incorporated but was distributed amongst the channels represented in models.

Figure 2: Effect of currents on simulated action potentials (APs) of PRd. The original AP as published (black). Addition of the TRPM4 current without any further modifications (green) resulted in a substantial APD prolongation. Additionally removing the equivalent current  $I_{Eqv}$  (red) produced an AP much closer to the original. Simulated block of the TRPM4 channel with 9-phenanthrol (blue), which is equivalent to only subtracting  $I_{Eqv}$  from the original model, resulted in a 29.1% reduction in APD.

The first step was to compute the expected TRPM4 channel current,  $I_{TRPM4}$ . This was calculated by applying the nominal model AP shape and  $Ca_i$  time trace (*i.e.*  $[Ca^{2+}]_{SSL}$ ) to the channel formulation at pacing cycle length (PCL)=1000 ms. Next, by analyzing kinetic profiles of the existing monovalent ion currents, a combination of these currents equivalent to  $I_{TRPM4}$  was determined. See Fig. 3 for the major monovalent ionic currents. The TRPM4 current had a constant component during the resting phase which could only be matched by the background sodium current,  $I_{Nab}$ , since all other inward currents were near zero. We assumed that all of  $I_{Nab}$  was composed of  $I_{TRPM4}$  and this allowed us to calibrate the conductance of  $I_{TRPM4}$ . The fitting was also constrained by considering that  $I_{TRPM4}$  could not be larger than the current component being replaced. Examining  $I_{TRPM4}$ , an initial large outward current was present which had to be  $K^+$  current, and the only possible current with that profile was transient-outward  $K^+$  current type 1 ( $I_{to1}$ ). In terms of magnitude, it was 10% of the initial  $I_{to1}$ . After adding this component to the equivalent current, the only candidate for matching the negative current during the AP plateau shape was the late sodium type 2 current,  $I_{NaL2}$ .

Figure 3: Major monovalent ionic currents for the Purkinje cell ionic model. Top: Original PRd model. Middle: Adjusted model with TRPM4 channel current and  $I_{Eqv}$  subtracted. Bottom:  $I_{TRPM4}$  is compared to  $I_{Eqv}$  and its constituent currents. The cell was stimulated at pacing cycle length (PCL)=1000 ms. Kr: rapidly activating delayed rectifier  $K^+$  current, NCX:  $Na^+-Ca^{2+}$  exchanger current, NaK:  $Na^+-K^+$  pump current, NaL2, NaL3: late  $Na^+$  currents, to1: transient outward current type 1 carried by  $K^+$ .

To capture the magnitude during the plateau, 33% of this current was added to the equivalent current. In summary, the best fit for the equivalent current,  $I_{Eqv}$ , was

$$I_{Eqv} = 0.1 \cdot I_{to1} + I_{Nab} + 0.33 \cdot I_{NaL2} \approx I_{TRPM4} \quad (11)$$

expressed in terms of the originally published currents (See Fig. 3 bottom). There was a small difference in currents during repolarization that could not be removed without reformulating kinetics of some current, so it was left out. For our new formulation,  $I_{Eqv}$  was removed from the original model by lowering the conductances of the selected channels, and the TRPM4 channel current added. This was verified by comparing the AP shape between models. The voltage trace was relatively preserved with an APD increase of 20.3 ms and a slowing in peak repolarization rate from -660 mV/ms to -534 mV/ms. Simulating block by 9-phenanthrol reduced APD by 29.1%, similar to that seen in rabbit Purkinje cells.

Table 1: Criteria for classifying cable behavior. Let  $A^x$  be the number of action potentials (APs) detected at node  $x$ , being the left (L), right (R) or middle (M) of the cable.  $N^P$  is the number of pulses delivered, and  $\Delta t_i^x$  is the delay between AP  $i$  at node  $x$  and the last pacing beat. Tests proceeded in order from top to bottom and stopped when the set of criteria were met.

Behavior	Criteria
1:1	$A^L = A^R = N^P \wedge \forall i : \Delta t_i^R \leq 40 \text{ ms}$
1 <sup>st</sup> degree block	$A^L = A^R = N^P$
Quiescent	$A^L = A^M = A^R = 0$
Pacemaker	$\exists x : A^x > N^P \vee \exists i : \Delta t_i^L > 2 \text{ ms}$
2 <sup>nd</sup> degree block	$A^L > A^R > 0$
3 <sup>rd</sup> degree block	$A^L > A^R = 0$
Repol. failure	$A^L < N^P \wedge A^R > 0$
Other	–

Rate dependence of APD and ionic concentrations in the cell (shown as max values of Na concentration in subsarcolemma ( $[Na^+]_{SSL}$ ), K concentration in the bulk myoplasm ( $[K^+]_i$ ) and spatially averaged  $Ca_i$  ( $[Ca^{2+}]_{avg}$ ) is similar to the original PRd without TRPM4 channels (Fig. 1B). Small differences occur at slow rates (PCL>1500 ms) and may be attributed to kinetic difference of TRPM4 current compared to  $I_{eqv}$ .

## Single Cell Upregulation

In a single cell, upregulation of TRPM4 channel expression lead to EADs at relatively modest increases (Fig. 4). This is not surprising given the large reduction in APD when it was removed. For increases above 2.12-fold nominal, the cells are no longer stable and repolarization failure render the cell unsuitable for propagation. In a mouse model of hypoxia and reoxygenation, pharmacological block of TRPM4 channel by 3-phenanthrol led to abolishment of EADs (18), indicating an important role of TRPM4 channels in EAD generation. For the slower PCL=1000 ms, EADs occurred with each beat. At short cycle lengths, EADs only occurred after rapid pacing stopped. However, during pacing the membrane voltage was rising just before the pacing beats were applied. It was quite different from resting potential.

Figure 4: Single cell action potential (AP) traces for varying levels of TRPM4 channel expression. Colors indicate TRPM4 channel expression. Blocking the channel leads to significant APD reduction (blue) compared to control (black). A 2.0-fold increase (green) considerably prolongs APD while a 2.1-fold increase (red) or more leads to early afterdepolarizations (EADs). Traces show last stimulated beats in a train of 30 at the indicated pacing cycle length (PCL).

## Cable Behavior

### Central Inhomogeneity

Activity in a 2 cm long cable was simulated using a finite element method with 100  $\mu\text{m}$  linear finite elements. The central portion of the cable (see Fig. 5A) had a different TRPM4 channel expression level than from the ends. The left end of the cable was paced with a transmembrane current stimulus at a PCL of either 600 or 1000 ms for 25s. APs were detected as excursions in transmembrane potential of at least 40 mV amplitude with an  $APD_{80}$  of at least 70 ms, and cable behavior was categorized by analyzing the last 22s of activity according to Table 1.

Figure 5: Cable simulations with central inhomogeneity. A: Cable strand showing TRPM4 channel expression level regions. The left and right regions expressed same levels. Pacing stimuli were applied to the leftmost end of the cable. B: Emergent behavior for different TRPM4 expression levels and Pacing Cycle Length (PCL) as indicated by color. See Table 1 for definitions.

For low levels of TRPM4 channel expression, the cable conducted every pacing pulse with an activation time of 30 ms. As TRPM4 channel expression was increased beyond doubling, single cells had repolarization abnormalities but the cells in the cable were still functional due to electronic effects of neighboring cells. First degree block occurred when the TRPM4 channel expression was increased in the midsection leading to a very slow propagation to the right end. Second degree block (see Fig.

6) was seen as TRPM4 channel expression continued to be increased in the midsection. In these cases, APs were not always present in the midsection although a low voltage appeared to passively propagate across the midsection which was sufficient to trigger an AP in the right end. Third degree block was seen only at the slower pacing rate. At both pacing rates, the system became quiescent with high TRPM4 channel expression. The resting levels depolarized to such a high level that  $Na^+$  channels could not regain excitability. With high TRPM4 channel expression levels in only one region (the ends or middle) pacemaking activity was also observed, more often at the slow pacing rate. Pacemaking activity was due to differences in resting potential level at the boundary between the high expression region and the low expression region. Due to electrotonic effects the region of lower resting potential could be excited by the region of higher resting potential to generate spontaneous APs. For homogenous TRPM4 channel expressions (along the main diagonal), the cable conducts 1:1 and then becomes quiescent.

Figure 6: Simulated transmembrane voltage recordings from the left, middle and right points of a Purkinje fibre. **A**: Quiescence (4,4,600), **B**: 1:1 (1,1,600), **C**: Type II block (1.5,4,600), **D**: Pacemaker from mid (1,4,1000), and **E**: Repolarization failure (4,0.5,600). Numbers in brackets indicate TRPM4 expression level at ends, in middle, and the pacing cycle length in ms, respectively. See Table 1 and Methods for definitions.

### Linear Gradient of TRPM4

We also implemented a linear gradient of TRPM4 channel expression in the same cable, stimulating again from the left end of the cable. The left and right ends were independently assigned expression levels from 0 to 5 times control levels with a linear gradient in between for PCLs of 600 and 1000 ms. For a left level of control channel expression or less, there was always 1:1 propagation regardless of the right TRPM4 channel expression levels. For left expression levels at or above 3.5 fold control expression level, there was no propagation in the cable. For a left end expression levels in the range 1.5-3 fold control, propagation only occurred when the right expression levels matched or exceeded the left end levels. APs at the right end under these conditions were normal, and those on the left end showed rhythmic subthreshold activity at a frequency faster than pacing frequency.

Figure 7: Cable simulations with a linear gradient of TRPM4 channel expression. Pacing stimuli were applied to the leftmost end of the cable, and the TRPM4 channel expression varied linearly in between. The emergent behavior for different TRPM4 channel expression levels and Pacing Cycle Length (PCL) are indicated by color. See Table 1 and Methods for definitions.

## DISCUSSION

We have made several assumptions regarding the TRPM4 channel formulation, regarding its reversal potential and its constituent currents. We have shown its formulation cannot be simply added to existing models so the channel must be already implicitly represented in the existing models. Based on channel current kinetics during AP, we decomposed it into background  $Na^+$ , transient outward  $K^+$ , and late  $Na^+$  currents. We assumed that all of background  $Na^+$  current in the original model was TRPM4 current, and used this to calibrate the channel conductance. When we calculated the APD reduction in the final model with channel block, it was close to that observed experimentally (13) (29.1 vs. 27%).

Based on the two spatial patterns of heterogeneity (linear and non-uniform TRPM4 expression along a cable) studied, it is found that a uniform high expression of TRPM4 channels will lead to quiescence. For propagation with a TRPM4 gain-of-function mutation, the region from which the pacing activity originates must have a lower expression level of TRPM4 than other regions. All degrees of heart blocks (Type 1, 2 and 3) were seen in the simulations, depending on the TRPM4 expression levels, but non-uniform heterogeneity was requisite for any behavior beyond quiescence and 1:1 propagation. With a linear gradient, the behavior observed was limited, being 1:1 propagation if the levels were low enough and for slightly higher levels, propagation if the gradient increased in the direction of propagation. First and second degree blocks were only seen with a non uniform TRPM4 expression in the form of central heterogeneity. The central region could act passively to propagate the AP, leading to either a significant propagation delay or second degree block. Interaction between two regions of different expression levels also led to pacemaking, although not always stable. The higher TRPM4 levels significantly depolarized the cells which in turn excited the neighboring cells electrotonically. With the central heterogeneity, activity was more diverse at faster heart rates.

Families with TRPM4 overexpression have exhibited higher tendencies to present with heart block (5). Simulations here are consistent with these observations. We can generate three degrees of block depending on TRPM4 expression profiles. For first and second degree block, there has to be a heterogeneity in Purkinje cable properties. This can occur by differential expression

of ion channels (eg. TRPM4 channels) in different regions of PF network. The TRPM4 current has a very large effect on APD; it is the second largest inward current during the plateau after  $I_{NaL2}$  and is the second largest outward current during phase 1. Thus global high expression, *i.e.*, greater than 3-fold control levels, would result in complete conduction failure of the His/Purkinje system. High expression levels have been estimated in patients with a TRPM4 mutation (5) but the spatial distribution was unknown. The propagation of electrical activity through the Purkinje system cannot be mapped but small branches may be blocked in these patients. Given the complex and redundant network, these blocks may not always be detectable, but bundle branch blocks have been observed and TRPM4 overexpression may explain it. For first and second degree blocks, the disruption would have to be quite proximal, in the His bundle, otherwise impulses from the atrio-ventricular node (AVN) could still arrive early in the ventricles. Cheng *et al.* (19) concluded that  $I_{Nab}$  in the AV node of rabbits was not TRPM4 current. However, the full expression profile of TRPM4 channels across tissue and species has yet to be performed, so we do not know if TRPM4 channels are in human AVN. In other tissues, TRPM4 channels may also be responsible, at least in part, for  $I_{Nab}$  current given its relatively large diastolic component. If human AVN is like rabbit AVN, this strengthens the argument that heart block observed clinically in patients with TRPM4 gain-of-function mutations, leading to its overexpression, are not due to AVN dysfunction since the channel is not present there, but rather due to propagation impairment in the fast conduction system. Thus, it is more probable that the heart block observed arises from failure of the proximal His/Purkinje fibres to conduct.

Our TRPM4 channel current was mostly attributed to the background  $Na^+$  current. Background currents exist in all ionic models for each ion, and are the currents for which no specific protein has been identified. They are necessary to balance ionic fluxes over the course of the AP. A background current may represent a portion of a nonselective cationic channel current, or several other currents which are not explicitly modeled. For example, the electrogenic glucose- $Na^+$  cotransporter-2 is usually not considered in electrophysiological models. Background currents are among the largest currents in cell models, as shown here, so if a new current is to be added to an existing ionic model, the background current must be adjusted or the behavior of the model will deviate markedly from what was intended. We also demonstrated that adjusting a background current may not be sufficient, especially for nonselective channels. Because TRPM4 channels are significantly permeable to  $K^+$  as well, a portion of an existing  $K^+$  current had to be removed. In this case, it was observed that the transient outward  $K^+$  current,  $I_{to1}$  fit the same kinetic profile. There are many more TRPM channels (20) which have been identified proteomically and characterized at the channel level. However, their functional consequences and correspondence with known currents in cardiac cells remain unelucidated. They may, indeed, underlie background currents found in other ionic models.

Our assignment of  $I_{Nab}$  to TRPM4 channels is in contrast to Cheng *et al.* (19) who found that TRPM4 channel was not responsible for  $I_{Nab}$  in mouse and rabbit atrioventricular node. However, expression of TRPM4 channels may differ across species and tissue type.

## Limitations

Our modeling study is based on PRd. Our result that  $I_{TRPM4}$  is implicitly a combination of  $I_{eqv}$  comprising of  $I_{Nab}$ ,  $I_{to1}$  and  $I_{NaL2}$  is specific to this model. In particular, it was observed that in PRd there is only one outward  $K^+$  current,  $I_{to1}$  during the phase 1 of AP and only one inward  $Na^+$  current during the plateau phase that can match the profile of experimentally based  $I_{TRPM4}$ . The conductance of  $I_{TRPM4}$  was determined by  $I_{Nab}$  during the resting phase. There may be more uncharacterized  $Na^+$  currents that can account for  $I_{Nab}$ . Other models of Purkinje cells may have more than one outward  $K^+$  currents or  $Na^+$  currents that match  $I_{TRPM4}$ . In that case a sensitivity analyses should be performed to determine the principal components of  $I_{TRPM4}$ . We have used a simple model of cable simulations of PF and TRPM4 overexpression. A more realistic model of PF network and a complex distribution of TRPM4 overexpression may lead to a different patterns of conduction abnormalities. However, our conclusion that heterogeneity of TRPM4 channel expression is required for intermittent heart blocks should still be valid in this case.

## CONCLUSION

In this work, we have developed a novel formulation of TRPM4 channel current using relevant experimental data. TRPM4 channel is activated by both voltage and  $Ca_i$  and can contribute significantly to the purkinje cell AP. We incorporated this channel into the PRd model of Purkinje cell by subtracting an equivalent current composed of  $I_{Nab}$ ,  $I_{NaL2}$  and  $I_{to1}$  to match the dynamics of TRPM4 current during the AP. The model formulation matches experimental data. Rate dependence of APD,  $Na^+$ ,  $K^+$  and  $Ca^{2+}$  concentrations of the PRd model with TRPM4 is a close match to the original PRd model values. Upregulation of TRPM4 channel leads to EADs in single cell. However, in cable only a heterogenous distribution of TRPM4 channels led to intermittent heart block, type II as seen clinically.

## AUTHOR CONTRIBUTIONS

NG designed and performed research, and wrote the manuscript. TH analyzed data, and wrote the manuscript. MH designed the research. EJV designed and performed the research, analyzed results and wrote the manuscript.

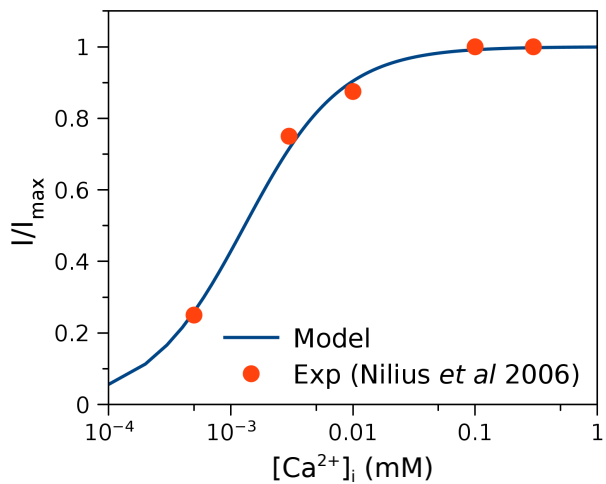
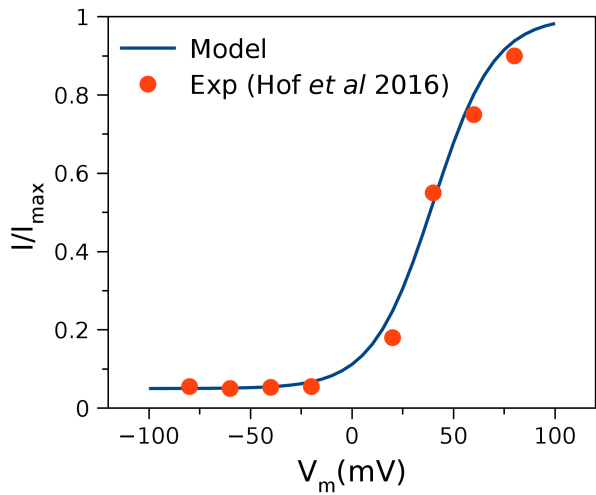
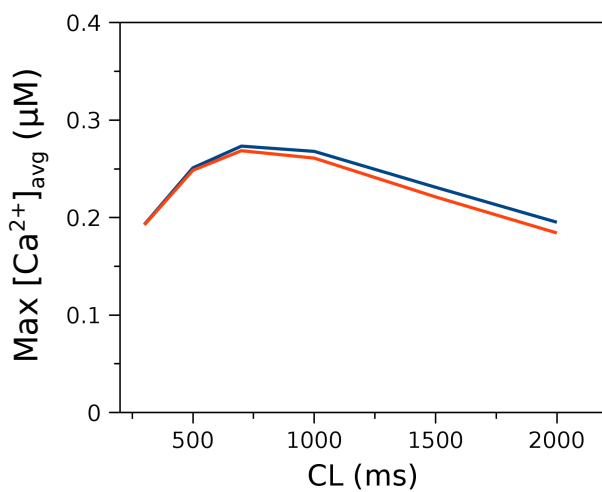
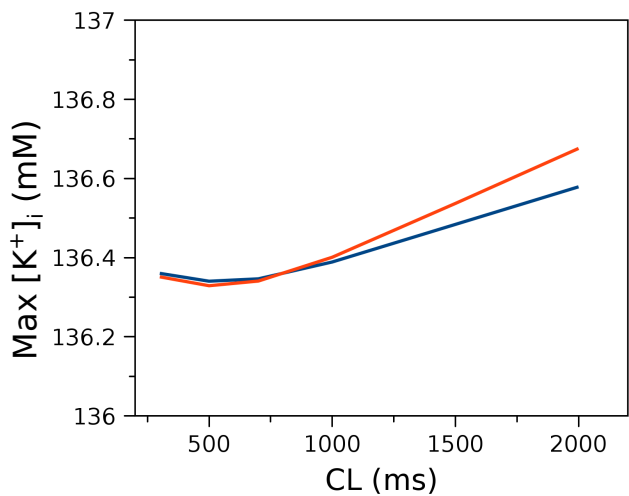
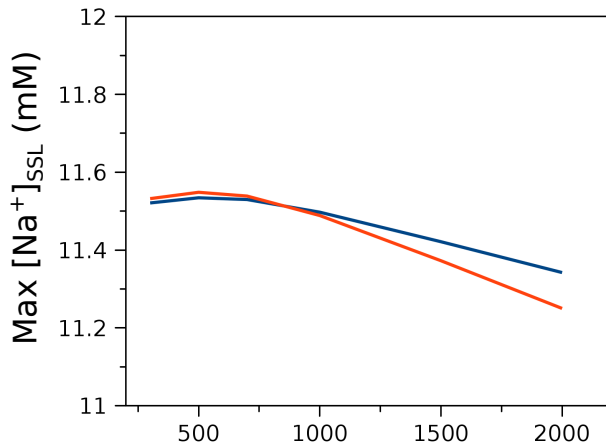
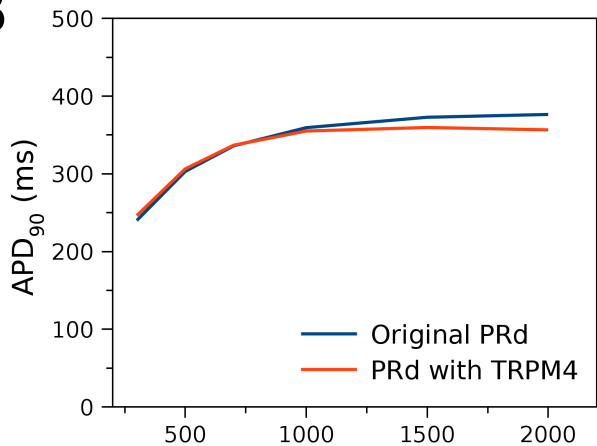
## ACKNOWLEDGMENTS

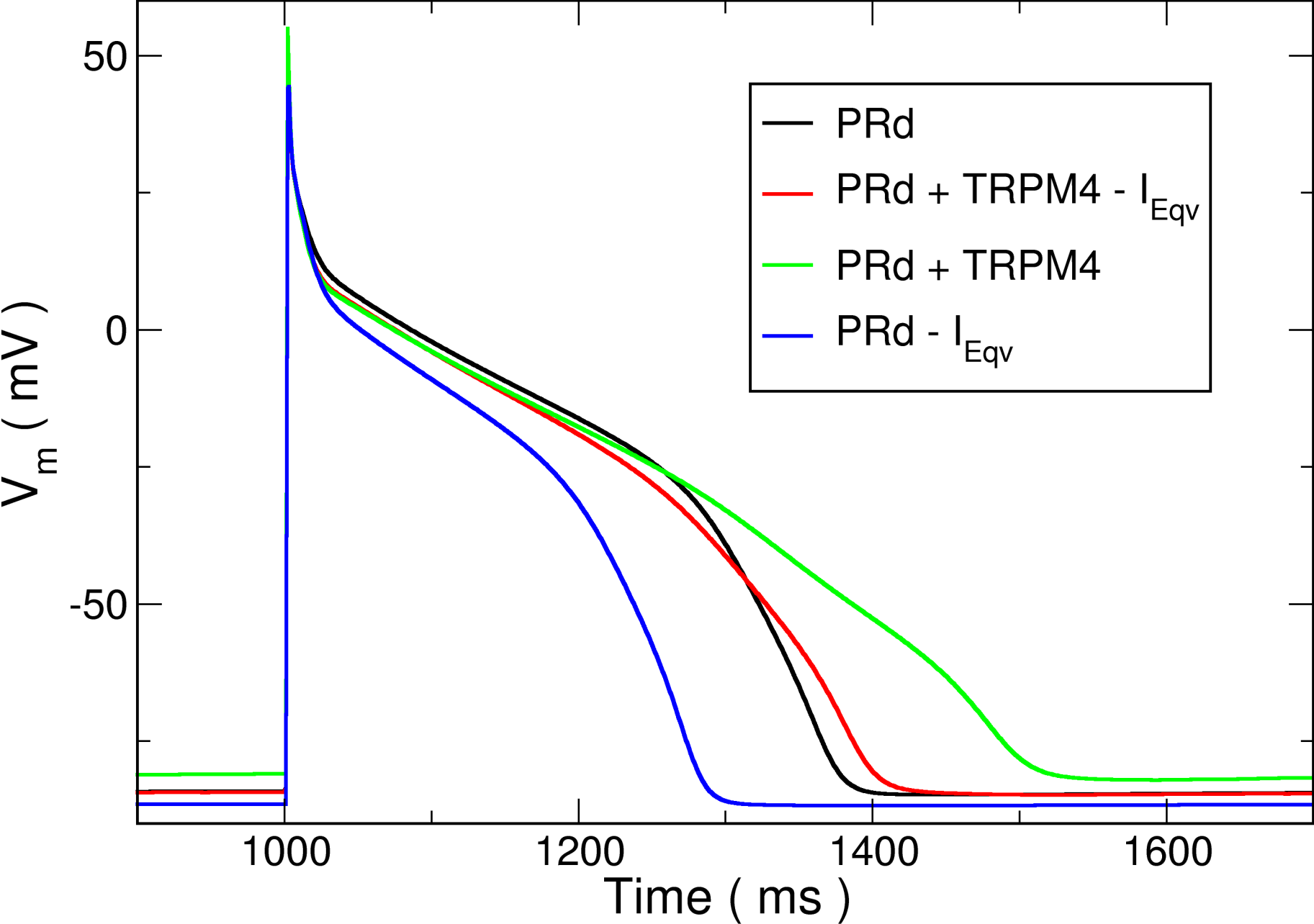
This study received financial support from the French Government as part of the Investments of the Future program managed by the National Research Agency (ANR), Grant reference ANR-10-IAHU-04. This project has received funding from the Fondation Leducq (Research Grant number 16 CVD 02) and the ERC (Symphony).

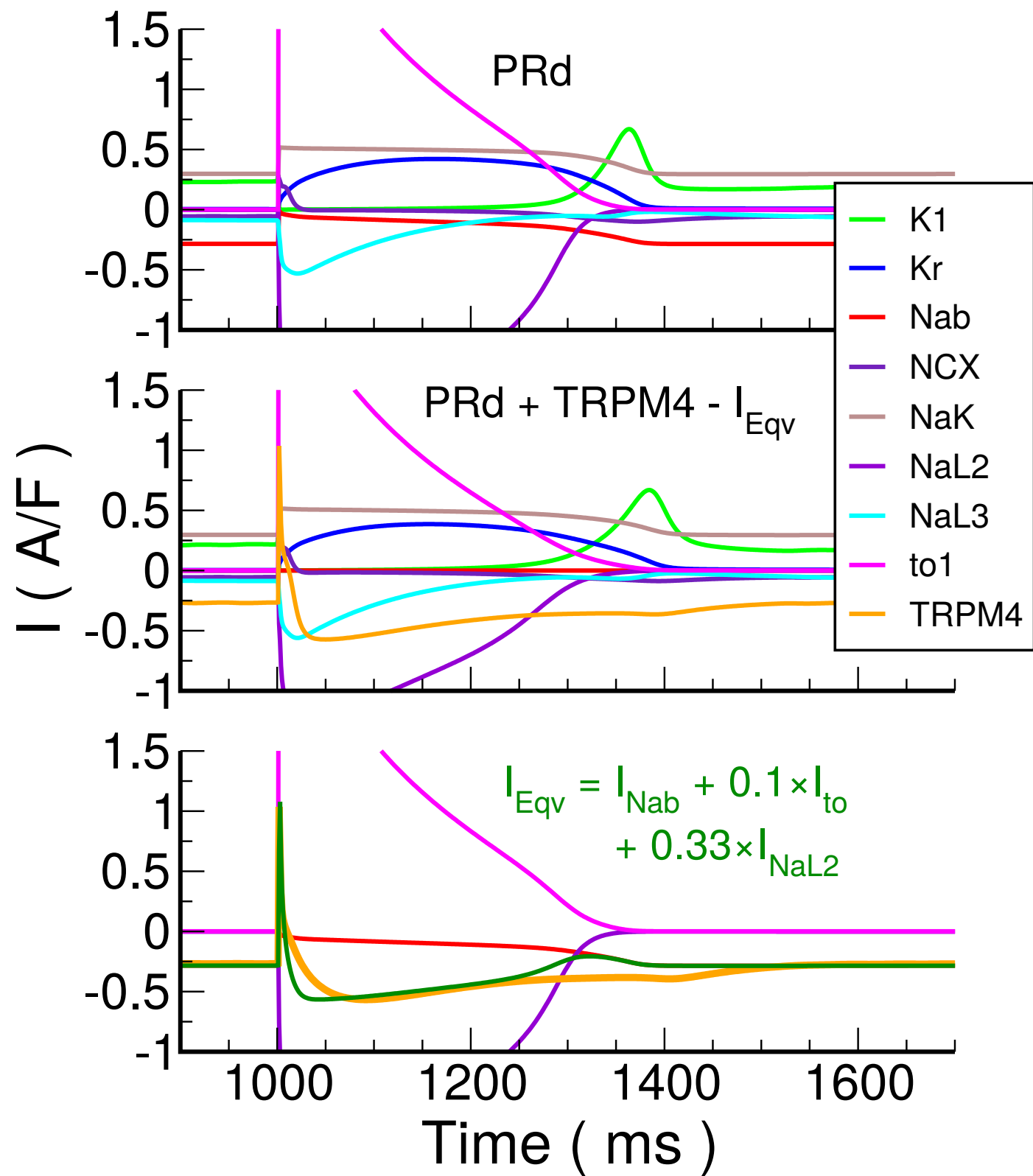
## REFERENCES

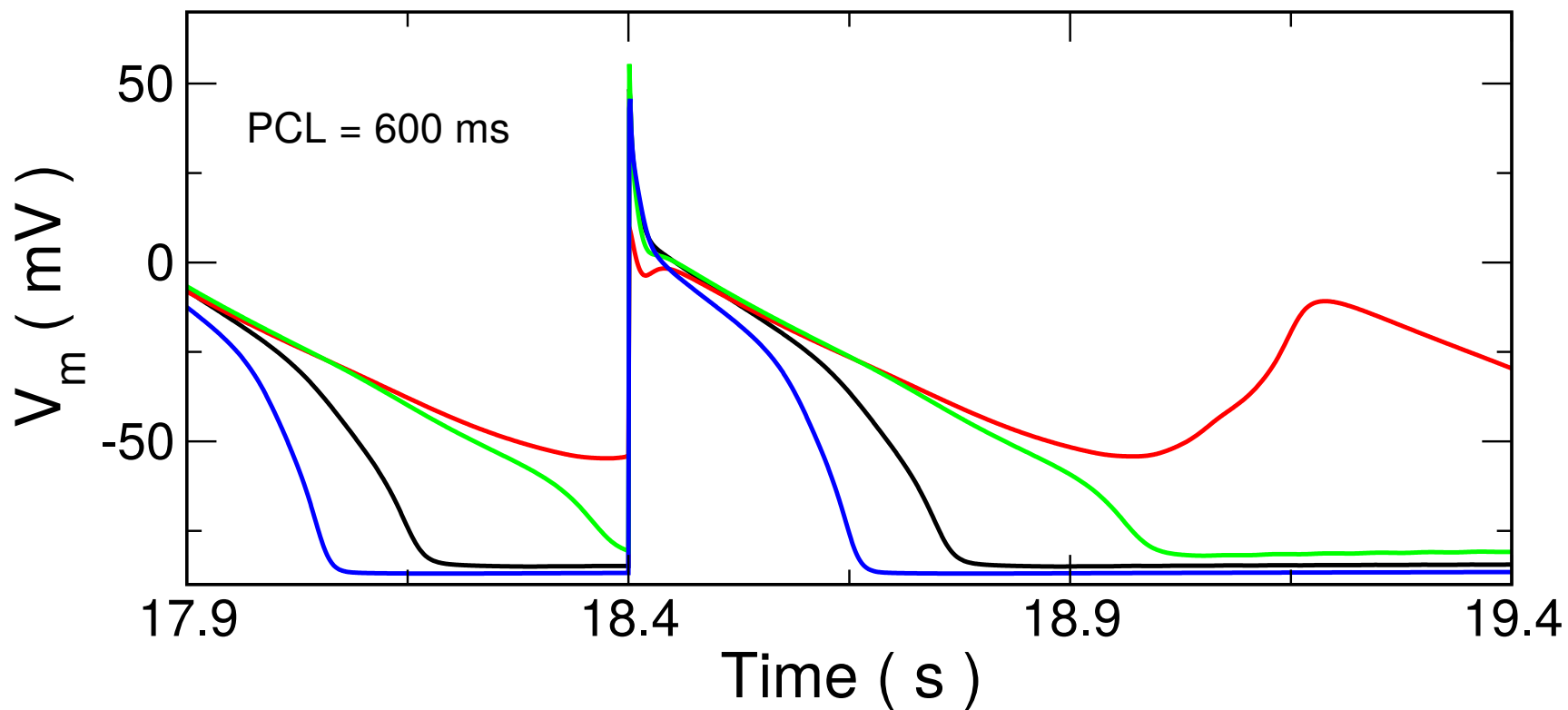
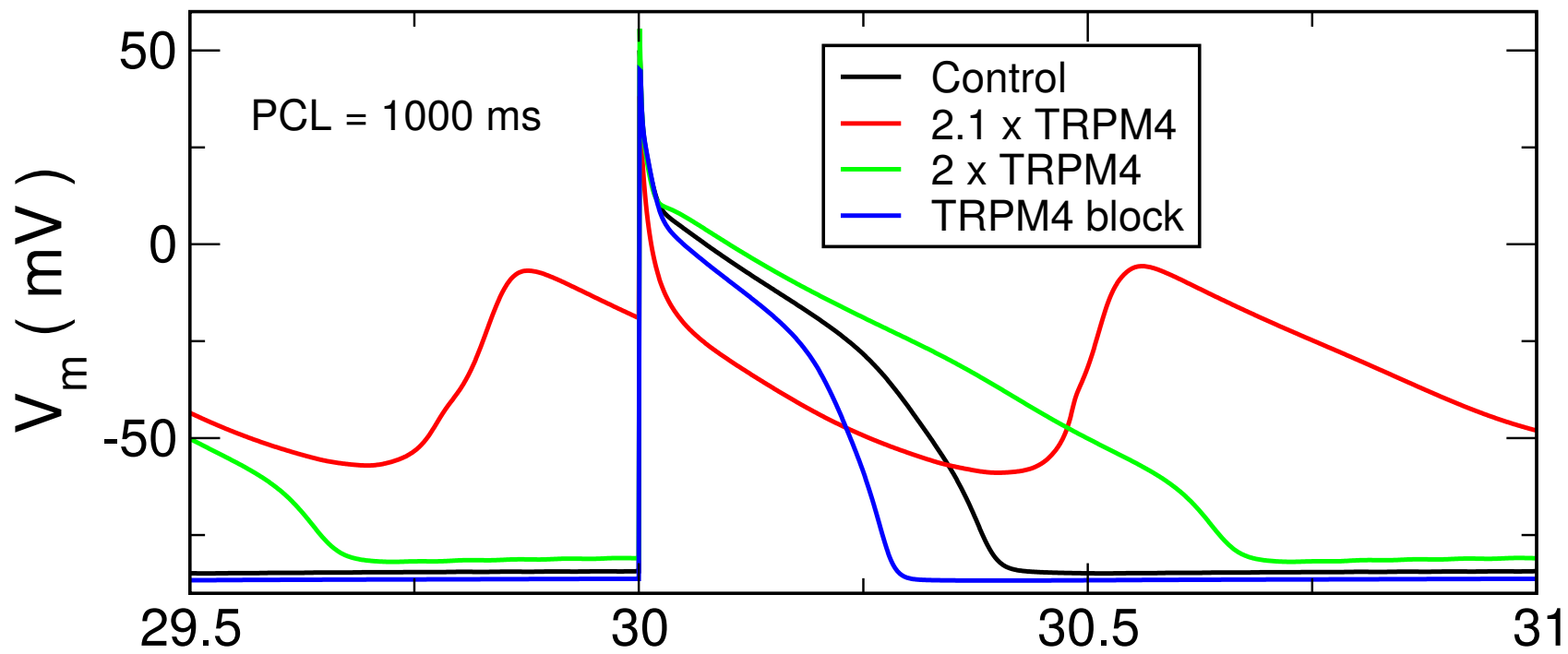
1. Launay, P., A. Fleig, A. L. Perraud, A. M. Scharenberg, R. Penner, and J. P. Kinet, 2002. TRPM4 is a Ca<sup>2+</sup>-activated nonselective cation channel mediating cell membrane depolarization. *Cell* 109:397–407.
2. Nilius, B., J. Prenen, A. Janssens, G. Owsianik, C. Wang, M. X. Zhu, and T. Voets, 2005. The selectivity filter of the cation channel TRPM4. *The Journal of biological chemistry* 280:22899–22906.
3. Guinamard, R., P. Bouvagnet, T. Hof, H. Liu, C. Simard, and L. Sallé, 2015. TRPM4 in cardiac electrical activity. *Cardiovascular research* 108:21–30.
4. Trafford, A. W., M. E. Díaz, S. C. O'Neill, and D. A. Eisner, 1995. Comparison of subsarcolemmal and bulk calcium concentration during spontaneous calcium release in rat ventricular myocytes. *The Journal of physiology* 488 ( Pt 3):577–586.
5. Kruse, M., and O. Pongs, 2014. TRPM4 channels in the cardiovascular system. *Current opinion in pharmacology* 15:68–73.
6. Kruse, M., E. Schulze-Bahr, V. Corfield, A. Beckmann, B. Stallmeyer, G. Kurtbay, I. Ohmert, E. Schulze-Bahr, P. Brink, and O. Pongs, 2009. Impaired endocytosis of the ion channel TRPM4 is associated with human progressive familial heart block type I. *The Journal of clinical investigation* 119:2737–2744.
7. Liu, H., L. El Zein, M. Kruse, R. Guinamard, A. Beckmann, A. Bozio, G. Kurtbay, A. Mégarbané, I. Ohmert, G. Blaysat, E. Villain, O. Pongs, and P. Bouvagnet, 2010. Gain-of-function mutations in TRPM4 cause autosomal dominant isolated cardiac conduction disease. *Circulation. Cardiovascular genetics* 3:374–385.
8. Saito, Y., K. Nakamura, N. Nishi, O. Igawa, M. Yoshida, T. Miyoshi, A. Watanabe, H. Morita, and H. Ito, 2018. Mutation in Patients With Ventricular Noncompaction and Cardiac Conduction Disease. *Circulation. Genomic and precision medicine* 11:e002103.
9. Syam, N., S. Chatel, L. C. Ozthail, V. Sottas, J.-S. Rougier, A. Baruteau, E. Baron, M.-Y. Amarouch, X. Daumy, V. Probst, J.-J. Schott, and H. Abriel, 2016. Variants of Transient Receptor Potential Melastatin Member 4 in Childhood Atrioventricular Block. *Journal of the American Heart Association* 5.
10. Xian, W., X. Hui, Q. Tian, H. Wang, A. Moretti, K.-L. Laugwitz, V. Flockerzi, S. Ruppenthal, and P. Lipp, 2018. Aberrant Deactivation-Induced Gain of Function in TRPM4 Mutant Is Associated with Human Cardiac Conduction Block. *Cell reports* 24:724–731.
11. Stallmeyer, B., S. Zumhagen, I. Denjoy, G. Duthoit, J.-L. Hébert, X. Ferrer, S. Maugendre, W. Schmitz, U. Kirchhefer, E. Schulze-Bahr, et al., 2012. Mutational spectrum in the Ca<sup>2+</sup>-activated cation channel gene TRPM4 in patients with cardiac conductance disturbances. *Human mutation* 33:109–117.
12. Li, P., and Y. Rudy, 2011. A model of canine purkinje cell electrophysiology and Ca(2+) cycling: rate dependence, triggered activity, and comparison to ventricular myocytes. *Circulation research* 109:71–79.
13. Hof, T., L. Sallé, L. Coulbault, R. Richer, J. Alexandre, R. Rouet, A. Manrique, and R. Guinamard, 2016. TRPM4 non-selective cation channels influence action potentials in rabbit Purkinje fibres. *The Journal of physiology* 594:295–306.
14. Nilius, B., J. Prenen, G. Droogmans, T. Voets, R. Vennekens, M. Freichel, U. Wissenbach, and V. Flockerzi, 2003. Voltage dependence of the Ca<sup>2+</sup>-activated cation channel TRPM4. *The Journal of biological chemistry* 278:30813–30820.

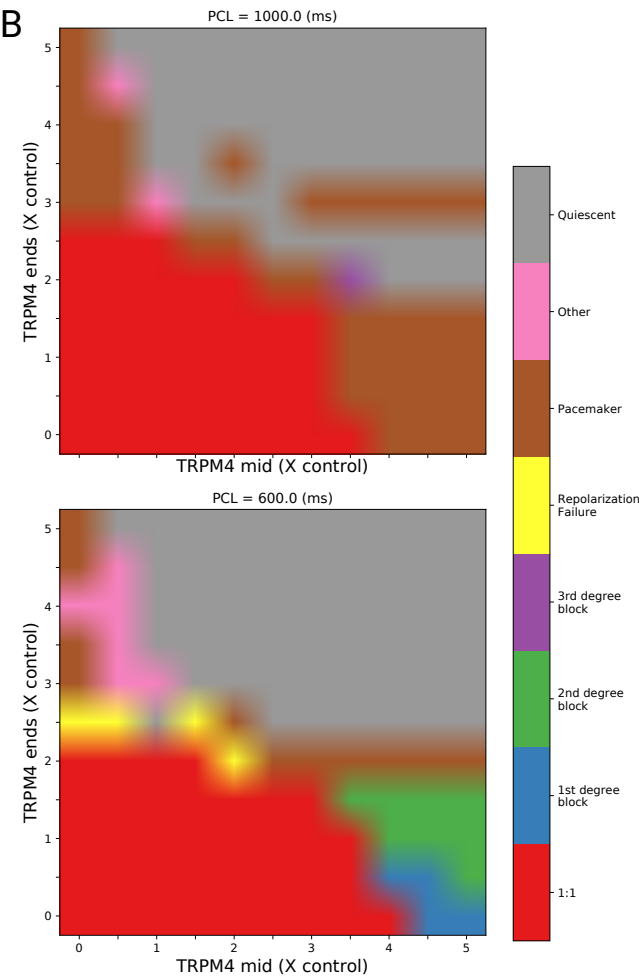
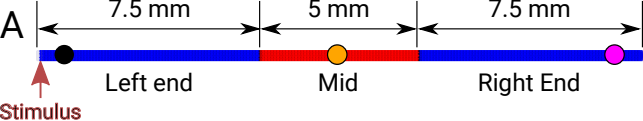
15. Nilius, B., F. Mahieu, J. Prenen, A. Janssens, G. Owsianik, R. Vennekens, and T. Voets, 2006. The Ca<sup>2+</sup>-activated cation channel TRPM4 is regulated by phosphatidylinositol 4,5-bisphosphate. *The EMBO journal* 25:467–478.
16. Vigmond, E. J., M. Hughes, G. Plank, and L. J. Leon, 2003. Computational tools for modeling electrical activity in cardiac tissue. *Journal of electrocardiology* 36 Suppl:69–74.
17. Hu, Y., Y. Duan, A. Takeuchi, L. Hai-Kurahara, J. Ichikawa, K. Hiraishi, T. Numata, H. Ohara, G. Iribe, M. Nakaya, M. X. Mori, S. Matsuoka, G. Ma, and R. Inoue, 2017. Uncovering the arrhythmogenic potential of TRPM4 activation in atrial-derived HL-1 cells using novel recording and numerical approaches. *Cardiovascular research* 113:1243–1255.
18. Simard, C., L. Sallé, R. Rouet, and R. Guinamard, 2012. Transient receptor potential melastatin 4 inhibitor 9-phenanthrol abolishes arrhythmias induced by hypoxia and re-oxygenation in mouse ventricle. *British journal of pharmacology* 165:2354–2364.
19. Cheng, H., J. Li, A. F. James, S. Inada, S. C. M. Choisy, C. H. Orchard, H. Zhang, M. R. Boyett, and J. C. Hancox, 2016. Characterization and influence of cardiac background sodium current in the atrioventricular node. *Journal of molecular and cellular cardiology* 97:114–124.
20. Yue, Z., J. Xie, A. S. Yu, J. Stock, J. Du, and L. Yue, 2015. Role of TRP channels in the cardiovascular system. *American journal of physiology. Heart and circulatory physiology* 308:H157–H182.

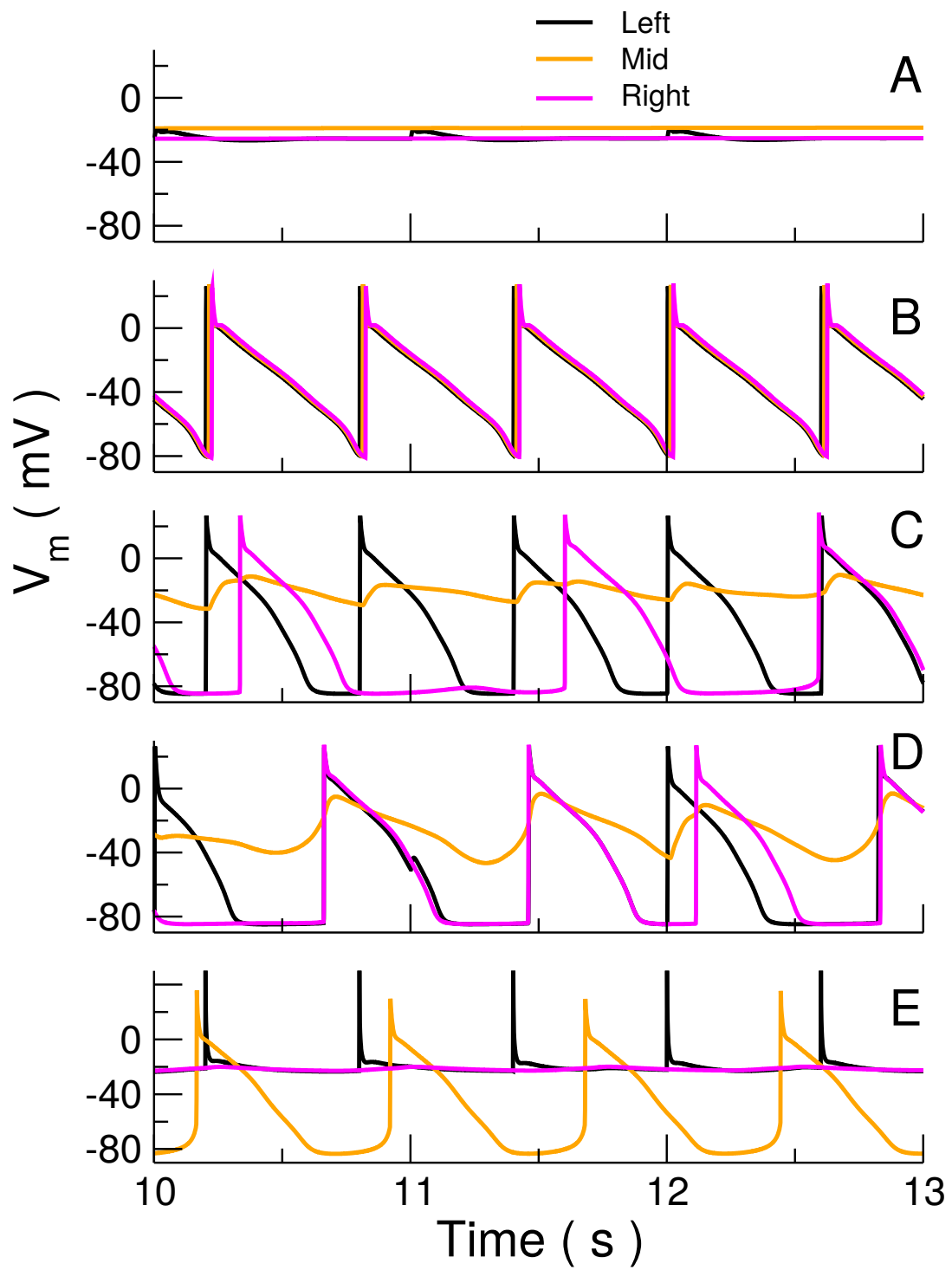
**A****B**



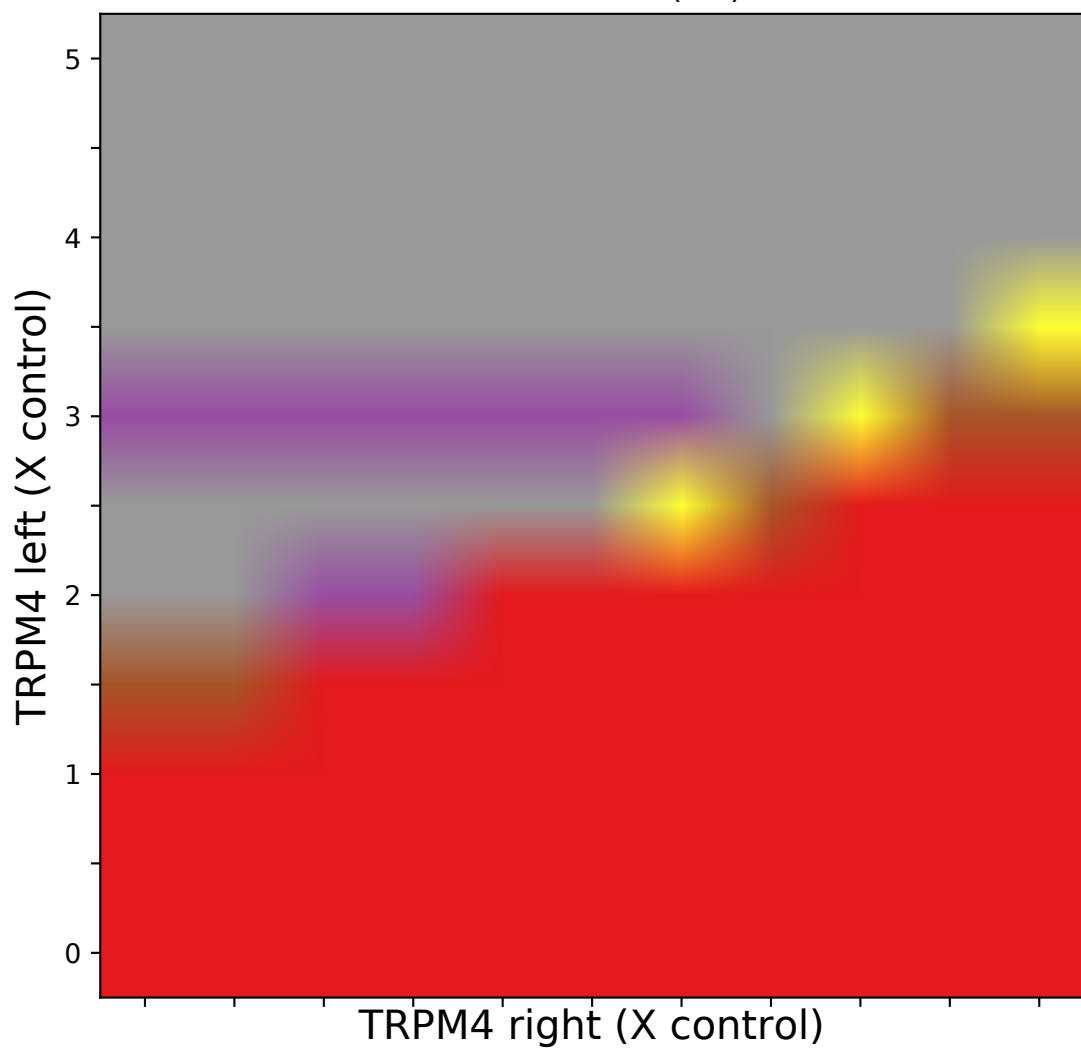






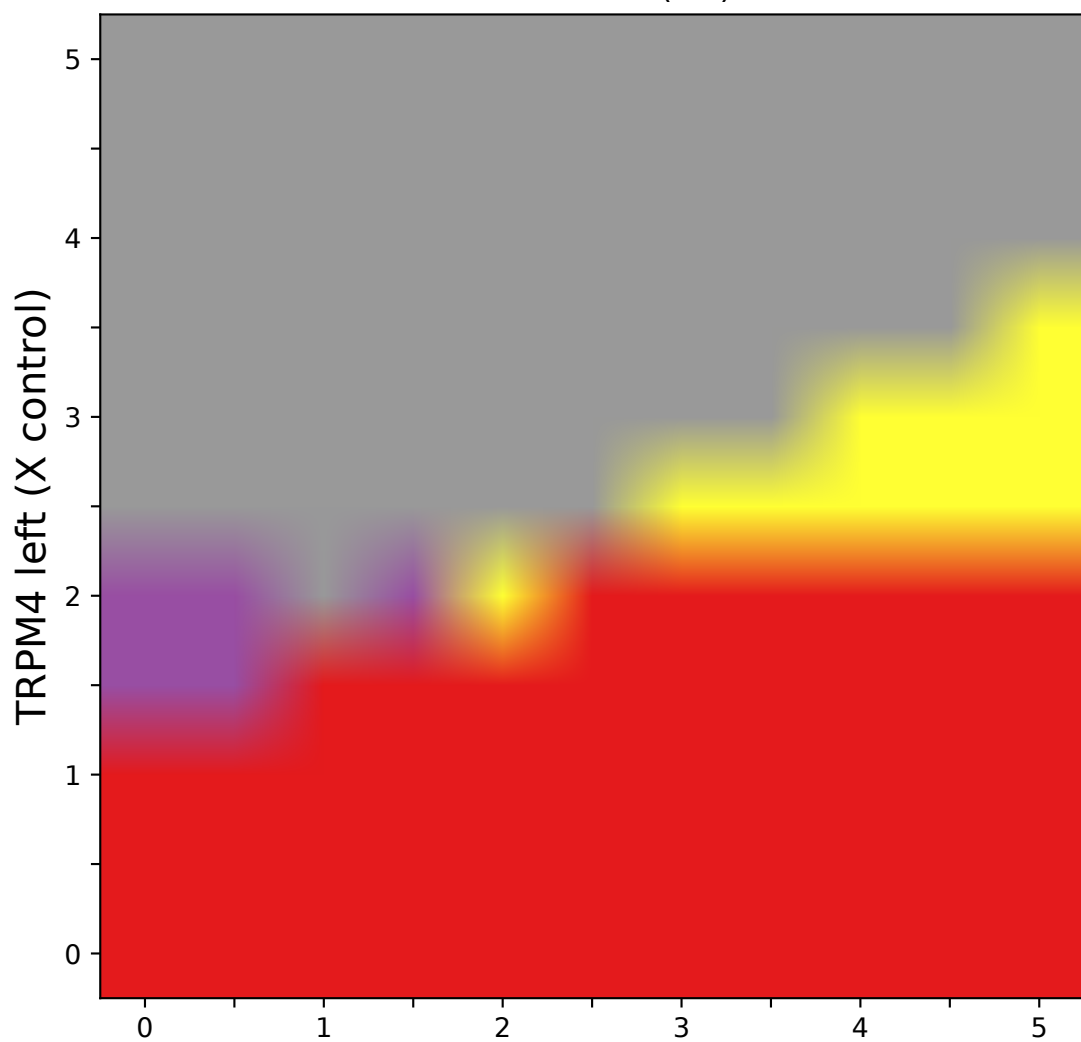


PCL = 1000.0 (ms)



TRPM4 right (X control)

PCL = 600.0 (ms)



TRPM4 right (X control)

